J. Cell. Mol. Med. Vol 16, No 6, 2012 pp. 1331-1341

Matrix metalloproteinase-1 contribution to sarcoma cell invasion

Nandor Garamszegi [a, b, *, #], Susanna P. Garamszegi [c], Sean P. Scully [a, d]

[a] *Sarcoma Biology Laboratory of Sylvester Comprehensive Cancer Center, University of Miami, Miller School of Medicine, FL, USA*
[b] *NAG-Biosystems, FL, USA*
[c] *Department of Neurology, University of Miami, Miller School of Medicine, FL, USA*
[d] *Department of Orthopaedics at University of Miami, Miller School of Medicine, FL, USA*

Received: April 20, 2011; Accepted: July 26, 2011

Abstract

Matrix metalloproteinase-1 (MMP-1) activity has been linked to numerous disease processes from arthritis to ulcer. Its proteolytic activity has been implicated inconsistently in different steps of tumourigenesis and metastasis. The discrepancies may be attributable to our limited understanding of MMP-1 production, cellular trafficking, secretion and local activation. Specifically, regulation of MMP-1 directional delivery *versus* its general extracellular matrix secretion is largely unknown. Inhibition of prenylation by farnesyl transferase inhibitor (FTI-276) decreased extracellular MMP-1 and subsequently reduced invasiveness by 30%. Parallel, stable cell line RNAi knockdown of MMP-1 confirmed its role in cellular invasiveness. The prenylation agonist farnesyl pyrophosphate (FPP) partially normalized FTI-276 inhibited extracellular MMP-1 levels and invasion capacity while transiently delayed its cellular podia distribution. MMP-1 directional delivery to these structures were confirmed by combination of a MMP-1–specific fluorogenic substrate, a MMP1-Ds-Red fusion protein construct expression and DQ-collagen degradation, which demonstrated coupling of directional delivery and activation. MetaMorph analysis of cellular lamellipodia structures indicated that FTI-276 inhibited formation and delivery to these structures. Farnesyl pyrophosphate partially restored lamellipodia area but not MMP-1 delivery under the time frame investigated. These results indicate that MMP-1 directional delivery to podia structures is involved in the invasive activity of sarcoma cells, and this process is prenylation sensitive.

Keywords: matrix metalloproteinase-1 • sarcoma • directional delivery • lamellipodia • invasion • prenylation

Introduction

Altered pericellular protease activity is a critical component of the metastatic cascade in many tumour types [1–5]. The protease activity that accompanies tumour invasion promotes cell migration by digesting physical barriers, exposing cryptic binding sites, liberating embedded growth/regulatory factors and simultaneously decreasing the availability of matrix adhesion ligands [6–8]. Cellular invasion correlates with matrix metalloproteinase-1 (MMP-1) expression in chondrosarcoma cells and transient down-regulation of MMP-1 expression decreases the cell invasion *in vitro* [1, 9, 10]. Despite the wealth of pre-clinical data implicating MMP-1 as a therapeutic target, the clinical trials with MMP inhibitors in cancer therapy provided disappointing results [11–13]. The reasons for this maybe several fold but likely include an attempt to indiscriminately inhibit a process that is not completely understood; namely, the regulation of MMP intra- and extracellular activity, production, delivery, compartmentalization and activation of this group of proteases [14].

Investigators have examined cancer cell migration and pericellular proteolysis with sophisticated imaging techniques [15,16]. They have demonstrated that MMPs are secreted in very specific pericellular locations and that these had biological and mechanical consequences for directed cell movement [17–20]. These studies support the contention that indiscriminate inhibition of MMPs determined the unsuccessful fate of previous clinical trials [11–13]. This interpretation led our laboratory and others to postulate that a more complete understanding of post-translational modification and delivery of MMPs would permit the development of a successful clinical strategy for novel MMP inhibitors [14].

Prenylation facilitates protein attachment to cell membrane [21]. It involves a 15-carbon farnesyl (FT) or 20-carbon geranylgeranyl (GGT) isoprenoid tag attachment to the target protein

[#]Present address: 9100 S Dadeland Blvd., STE 1500 Miami, FL 33156, USA.
*Correspondence to: Nandor GARAMSZEGI,
University of Miami, Miller School of Medicine,
M877 Papanicolau Building Room 315,
1550 N.W. 10th Avenue, Miami, FL 33136, USA.
Tel.: 305-243-6329
Fax: 305-243-9445
E-mail: ngaramszegi@med.miami.edu, sunag101@gmail.com

doi:10.1111/j.1582-4934.2011.01402.x

carboxyl-terminal cysteine residues on preferred CAAX target sequences. This process is catalysed by enzyme complexes termed protein farnesyltransferase (FTase) and protein geranylgeranyltransferase type I and II (GGTase-I and II) [22–25]. Inhibition of prenylation has been explored as an anti-neoplastic strategy in various cancers, affecting numerous cellular processes and signalling cascades including Ras [26–29]. Prenylation inhibitors have also been reported to disrupt subcellular trafficking of proteins within cells [30]. These interventions reduced tumour burden and induced apoptosis *in vitro* and in pre-clinical models [31,32]. The specific mechanisms for the observed anti-neoplastic effects were unclear because of the breadth of protein targets of prenylation [33–37]. Recently investigators have reported that in rheumatoid arthritis, MMP-1 secretion from synovial tissue could be inhibited by blocking prenylation [38]. The study did not specifically investigate the effect of inhibition on MMP-1 subcellular delivery, documenting only affects on general secretion. It should be noted that MMP-1 by itself is not prenylated (there is no existence of suitable carboxyl-terminal target sequence). Based on what is known about prenylation and protein trafficking, inhibition of MMP-1 directional traffic is likely to have important effects on cell migration and tumour invasion particularly in human chondrosarcoma [39–42].

This study demonstrates that the ability of a cell to invade a collagen barrier is partially related to MMP-1 delivery to podia structures. Inhibition of prenylation affects lamellipodia formation, MMP-1 localization into these structures and secretion. The lamellipodia formation can be partially restored by the prenylation agonist farnesyl pyrophosphate (FPP), while MMP-1 delivery to these structures delayed under the time frame investigated. This study seeks to understand the intracellular directional delivery of MMP-1 in support of a better devised and targeted approach to MMP inhibition.

Materials and methods

Cell culture and inhibition of prenylation

Human osteogenic sarcoma cells (143B, CRL-8303; ATCC Bethesda, MD, USA) were cultured in DMEM (#10-017CV; Invitrogen, Carlsbad, CA, USA) complemented with 10% foetal bovine serum (FBS). After trypsinization, cells were quenched in DMEM with 5% bovine serum albumin then incubated overnight in p100 plates at 37°C to achieve a 70% confluence before serum starvation. Next FTI-276 {15 μM, [4-[2-(*R*)-amino-3-mercaptopropyl] amino-2-phenylbenzoyl] methionine trifluoroacetate salt, #F9553; Sigma-Aldrich, St. Louis, MO, USA} and/or its antagonists FPP (20 μM, 3,7, 11-Trimethyl-2,6,10-dodecatrien-1-yl pyrophosphate ammonium salt, #F6892; Sigma-Aldrich) alone, or in combination of two were used in serum-free DMEM overnight. Following exposure, cells were washed with PBS and harvested on ice. Samples either were processed immediately or snap frozen in liquid N_2 and stored at −80°C until further use.

Generation of stable RNAi clones

Stable clones were generated by pHuSH 29mer shRNA constructs targeting MMP-1 (#TR311450; OriGene, Rockville, MD, USA) and established by puromycin selection (Invitrogen; 1.0 μg/ml in the media above) on six-well plates. The RNAi kit composed of three separated targeting sequences and a negative control. Individual colonies were isolated through parallel process, expanded in selection media containing the antibiotics until passage was transferred into p100 plates. Then the antibiotic was removed, and colonies were screened for gene expression changes by RT-qPCR. The screening process was repeated at least three to five times with every second passages to establish the stability of down-regulation. Clones used in this study were designated as T6-4, T6-5 and T6-7.

Collagen-based cell invasion assays

QCM™ 96-well collagen-based cell invasion assay from Chemicon International (#ECM556) was used. Coatings on the plates were avian collagens Type I (85%) and Type III (15%), respectively. Assays were performed according to the protocol's manual with the following modifications: after initial cell number normalization, 4.0×10^4 cells/well was seeded onto the plates (nine parallels with three blank controls) in media combined with pharmacologic agents (untreated controls, FTI-276, FPP, FTI-276/FPP). Feeder wells contained the same media ± 10% FBS to determine the effects of natural metalloproteinase inhibitors and incubated overnight. The following day the plates were processed according to the Chemicon's protocol then measured with 480/520 nm filter set on Berthold Mithras LB 970 plate reader. The data were transferred into Microsoft Excel for further statistical analysis (ANOVA; where the null hypothesis is that conditions are different and confirmed when $P < 0.05$) and graphing.

Three-dimensional collagen gel matrices and invadopodia assay

One packet of alpha Minimal Essential Medium (α-MEM, #11900-073; Invitrogen) was dissolved in 100 ml of endotoxin-free, distilled water to bring the medium concentration to 10-fold. 2.2 g of sodium bicarbonate was added to neutralize the media. Purcol acidified collagen (97% Type I collagen/3% Type III collagen, 3.0 mg/ml, #5409; INAMED Corporation, Santa Barbara CA, USA) was aliquoted into 15 ml conical tubes for individual use. Subsequently, collagen gels were mixed in the following proportions: 1000 μl Purcol Collagen, 125 μl α-MEM and 175 μl DQ Collagen (#D12060; Invitrogen). The solution was neutralized to pH 7.0 by the addition of 0.8M sodium bicarbonate prepared in endotoxin-free distilled water. Gels were cross-linked with 0.3% glutaraldehyde/PBS to the cover slips (5 min. at room temperature and 15 min. on ice). Total gel volume of 70 μl was used with 12-mm circular cover slips (polymerized on parafilm upside down) to standardize its thickness to ~80–100 μm. Gels were then seeded at 2.5×10^4 cells/ml/well concentration. For lamellipodia MMP-1–specific activity studies, Fluorogenic MMP1-Substrate-III (#444219; Calbiochem, EMD Biosciences, Gibbstown NJ, USA) was used (1 mg/ml) to saturate the gels. The MatTek dishes (P35G-1.0-14-C) were prepared as described [43–45] with 150 μl of matrix mixture. Excess was aspirated and dishes dried in dark for 30 min. followed by cross-linking with 2 ml of 0.5% glutaraldehyde/PBS (chilled in ice) and incubated on ice for 15 min., then at room temperature for 30 min. Second coating with MMP-1 cleavage specific Fluorogenic Substrate-III was used to saturate the cross-linked gels. The equilibrated dishes (OptiMEM media, 1% FBS serum) were stored at 4°C in dark until use. Cell growth, MMP-1 breakdown of DQ-collagen, and MMP1-S-III substrate degradation were observed with Zeiss Axioplan II fluorescent microscope with 40× objective with DAPI (blue), GFP (green)

and DsRed (orange) filters combined with PlasDIC filter (transmitted light and merge) to collect live cell images.

Western blotting, image acquisition and statistical analysis

Extracellular media was separated from cells by centrifugation and retain for determination of MMP-1. Cells were then lysed in buffer containing 50 mM Tris–HCl pH 7.4, 1% NP-40, 0.25% Na-deoxycholate, 150 mM NaCl, 1 mM EDTA, 1 mM Na-vanadate and 1 mM phenylmethylsulfonyl fluoride, completed with protease inhibitor cocktail from Roche (Indianapolis, IN, USA). Samples were normalized for protein content with ND-1000 (NanoDrop Technologies Inc., Wilmington, DE, USA). For Western blotting, 125 μg protein samples per lane were analysed with primary antibodies [MMP-1 #sc-58377, farnesyltransferase, CAAX box, alpha (FNTA) #sc-136, actin #sc-1615; Santa Cruz Biotechnology Inc. (Santa Cruz, CA, USA), and #610002; BD Biosciences (San Jose, CA, USA)], incubated overnight at 4°C, followed by secondary HRP conjugated antibodies (Amersham/GE, Piscataway, NJ, USA) for 1 hr at room temperature. Bands were detected with SuperSignal West Pico ECL detection kit (Pierce, Rockford, IL, USA) on UVP Biospectrum Digital Imaging System (UVP Inc., Upland, CA, USA). Raw images were quantized by optical density through supplied densitometry analysis software. Data were transferred to Excel file and statistical analysis was performed by the ANOVA subroutine of Microsoft Excel and/or MATLAB 7.5.0 software (The MathWorks, Inc., Natick, MA, USA) to verify the significance of densitometry results (0 hypothesis that they are different when $P < 0.05$).

Real-time quantitative PCR

Total RNAs were purified with RNeasy Mini Kit with on column DNase treatment (Qiagen Inc., Valencia, CA, USA) according to the manufacturer's protocol. For the cDNA synthesis, 5 μg total RNA was used with High Capacity cDNA Reverse Transcription Kit (#4368813; Applied Biosystems, Foster City, CA, USA) as described by the kit manual. All genes were analysed in triplicate in 20 μl mixture/well containing 100 ng cDNA and 2 TaqMan Fast Universal PCR Master Mix (#4352042; Applied Biosystems). 18S was used as the internal control. Relative RT-qPCR was performed on AB 7900HT Fast Real-Time System using specific human TaqMan gene expression assays MMP-1 (#Hs00233958_m1), TIMP1 (#Hs00171558_m1), KRAS (#Hs00364282_m1), FNTA (#Hs00357739_m1). Relative quantities of each gene were determined by the manufacturer's default ΔΔCt method.

Fluorescent microscopy and MetaMorph analysis

Cells were plated in four chamber slides (Lab-Tek 1177399, Nalgene-Nunc Int., Rochester, NY, USA) at density of (2.5–3.0) $\times 10^4$ cells/chamber and then were grown to confluence overnight. Following exposure to prenylation inhibitors, cells were washed with PBS then fixed by 4% formaldehyde and processed according to standard immunostaining protocols. Cells were stained with primary antibody against MMP-1 (#sc-21731; Santa Cruz), counterstained with DAPI (#D21490) and AL647-Phalloidin (#A-22287) both from Invitrogen (Molecular Probes, Eugene, OR, USA) for nuclei and F-actin respectively. The secondary antibody against MMP-1 was AL594 (#A-21201) from Molecular Probes. Slides were mounted in ProLong (#P-7481; Molecular Probes) then imaged with Zeiss LSM 510 confocal microscope at Sylvester Comprehensive Cancer Center Bioimaging Core. Above from the blue, red and far-red (pseudo-coloured as white) channels, reflected interference images from the cover-slips were collected to aid in the determination of lamellipodia regions of the migrating cells. Confocal z-sections were combined and the resulted images were depth-coded to visualize better the lamellar regions. Red channel was extracted from the images then total and partial red pixel counts were performed to determine the total MMP-1 levels as well as its localization to lamellipodia structures. Interference image of same cells with pseudo-coloured intensity levels of MMP-1 (red channel) were depth-coded and used to determine the boundaries of lamellipodia structures. These regions were marked and numbered in each cell for subsequent pixel counts.

For MetaMorph analysis, the image background was subtracted in the software by threshold binary processing. Then lamellipodia regions were outlined (according to the previously depth-coded image), and numbered in the software. Data were logged by total cell count and region measurement command (lamellipodia pixel count) into Microsoft Excel spreadsheet. MMP-1 lamellipodia localization and surface area were then related to total cellular MMP-1 and total cell surface and expressed as its percentage. The counts were performed on 30–50 cells from each condition (untreated, FTI, FPP and FTI/FPP). For lamellipodia studies, MMP1-Substrate III (excitation/emission = λ 365/450 nm) was recorded with live cells at ~461 nm (DAPI channel) with Zeiss Axioplan II microscope (40× objective). MMP-1 cleavage was quantized in the podia structures of 45–50 cells for each condition through the blue channel.

Results

Cellular invasiveness is affected by farnesyl transferase inhibitor (FTI)

To investigate how cellular transport of MMP-1 affected tumour cell invasion *in vitro*, we used a prenylation inhibitor (FTI-276) which inactivates the FTase (composed of A and B subunits termed FNTA/FNTB) complex by blocking the active site of the FTase enzyme [46]. To examine the efficacy and specificity of the FT inhibition, cytoplasmic Ras was used as an MMP-1-independent surrogate marker (Fig. 1A, second row). FTI-276 prevents Ras farnesylation, efficiently blocking its plasma membrane translocation and consequentially increasing cytoplasmic concentration. Effects of FTI-276 on both Ras cytoplasmic and extracellular MMP-1 levels are noted between 5 and 15 μM, correlating with inhibition of FTase activity up to 50 μM, indicating that the overall secretion process is prenylation dependent (Fig. 1A). Corresponding transmembrane cellular invasion is decreased 25% by FTI-276 consistent with the inhibition of secretion. FPP (FNTA substrate and prenylation agonist) is able to overcome FNTA inhibition and restore the invasion up to ~85% to its original levels, indicating that reversal of FT inhibition is associated with partially restored cell function (Fig. 1B). Effects of FTI-276 and FPP were significantly different (ANOVA, $P = 0.001$), and null hypothesis confirmed P-value >0.05 would indicate no difference.

Farnesyl transferase inhibition decreases MMP-1 extracellular protein levels by 35% and this effect is reversed by FPP to 82%

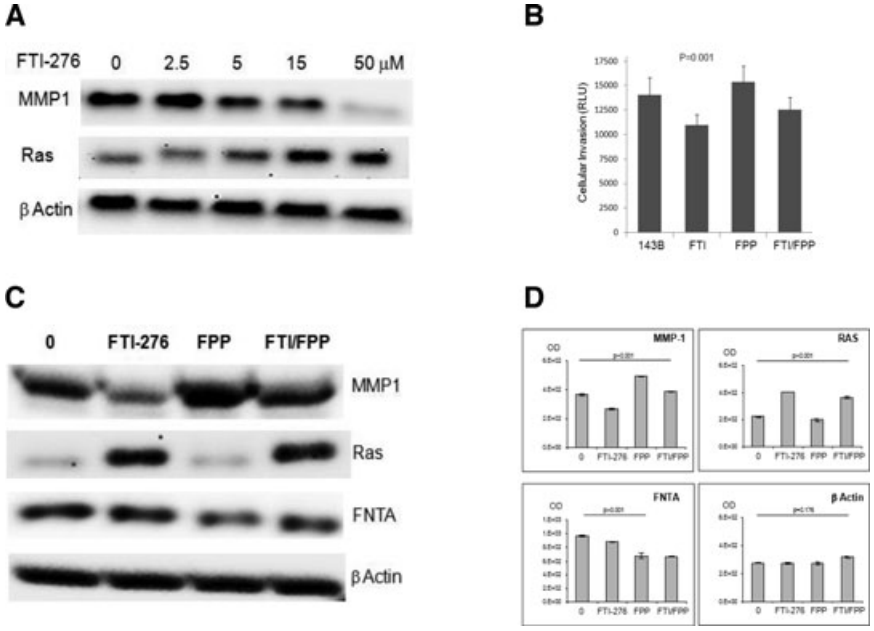

Fig. 1 Cell invasion was affected by farnesyl transferase inhibitor. (**A**) FTI-276 concentration effect on extracellular MMP-1 protein levels. Pan-Ras antibody was used to show that the drug is working and β actin employed as loading control. (**B**) Cellular invasion through a transmembrane collagen matrix down-regulated by FTI-276. Blanks (no cells) were used as controls. The invasive behaviour of parental 143B cells were significantly affected by FTI and FPP, while their combination partially normalized the activity (FT/FP). *Y*-axis measures cells that migrated through the transwell as described under the Materials and Methods section in reporter light units (RLU). (**C**) Extracellular MMP-1 was affected by FTI-276 and FPP. The extracellular MMP-1 protein level is displayed. The cellular FNTA levels demonstrate that the inhibitor does not alter the FTase subunit concentration and pan-Ras antibody was employed to validate efficacy of the inhibitor. Actin is the loading control. (**D**) Raw digital Western blot images show highly significant differences with $P < 0.001$ values for all bands analysed, except for the loading control (actin, $P = 0.176$).

(Fig. 1C). FPP alone causes a 20% increase in MMP-1 extracellular protein and leave cytoplasmic Ras levels unchanged (Fig. 1D, relevant Western blots quantization, *Y*-axis in optical density). Notably, the addition of FPP- to FTI-276–inhibited cells did not reverse cytoplasmic Ras accumulation and MMP-1 levels were less than FPP alone. These changes were not associated with significant changes in the levels of FNTA or β-actin.

MMP-1 RNAi validation of FTI affect on cellular invasion

The question arose as to whether the observed alterations in the extracellular MMP-1 protein levels induced by prenylation inhibition are reflected merely protein export or whether there is an associated change in gene expression too (Fig. 2A). FTI-276 down-regulated MMP-1 gene expression by 29.84% and up-regulated Ras mRNA levels by 23.42% (used only as indicator of the inhibitor effectiveness at mRNA level). TIMP1 (a natural MMP-1 inhibitor) is demonstrates parallel changes with MMP-1 gene expression. FNTA expression was not affected significantly by prenylation inhibition or substrate excess. Differential magnitude of changes between gene expression and secretion indicate that they might be guided by different kinetics. To validate further, the MMP-1 contribution to cellular invasiveness OriGene pHuSH targeting MMP-1 constructs were used to establish three parallel stable cell lines (143B cells; Fig. 2B). Following the selection process, clones showing over 80% stable MMP-1 down-regulation were designated as T6-4, T6-5 and T6-7. Targeting specificity was confirmed through MMP-14 (MT-MMP1), which importantly also associated with the invasion process. It was slightly up-regulated in two clones and down-regulated (~30%) in T6-7. This slight up-regulation did not rescue the MMP-1 knockdown effect on the cellular invasiveness (Fig. 2D). MMP-1 protein expression levels confirm the RT-qPCR analysis (Fig. 2C). Here the equal loading was confirmed by β-actin. Over 80% of MMP-1 mRNA down-regulation at the gene expressional level in all three clones (Fig. 2B) was responsible for ~50% decrease in trans-membrane invasion/migratory capacity (Fig. 2D; ANOVA, $P < 0.001$; T6-4 and T6-7 invasion levels statistically similar, $P = 0.129$).

MMP-1 cellular lamellipodia distribution is FTI sensitive

Cellular transmembrane invasion reflects and measures invadopodia-related MMP activity and matrix degradation. The observed MMP-1 contribution to *in situ* invasion results between RNAi interference and FTI-276 treatment (Figs 1 and 2) raised the possibility that sub-cellular distribution of MMP-1 might be an important component of the invasive mechanism(s). To further understand the relationship between MMP-1 localization and invasion, we examined how FNTA inhibition affects cell morphology. First, to determine the extent of the lamellipodia for each cell (Fig. 3A), the cells were evaluated with fluorescence microscopy. Image analysis was aided by DAPI staining to locate the cell nucleus and

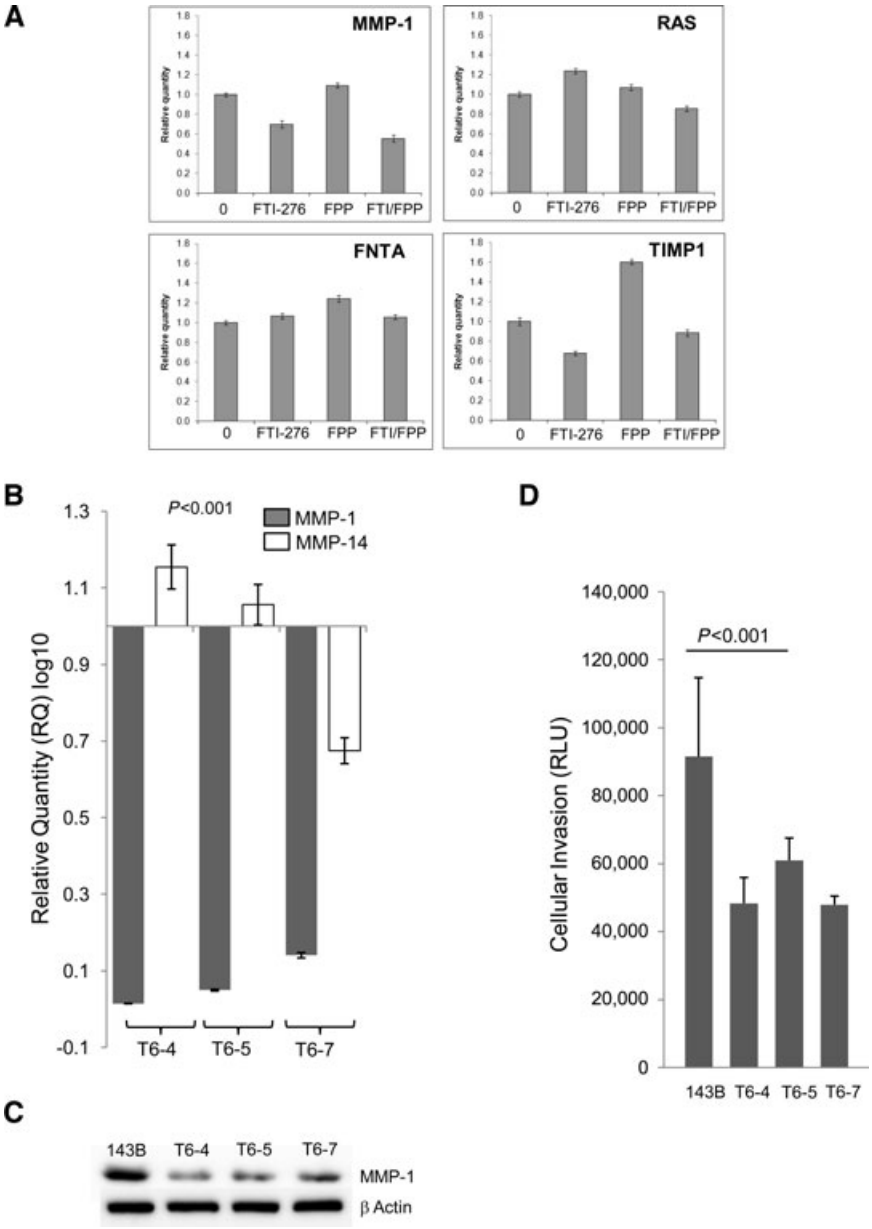

Fig. 2 Validation of drug responses by real-time quantitative PCR method. (**A**) Expressional mRNA levels of target molecules. Relative quantity (RQ log10) values reflect changes from untreated control samples (gene expression levels = 100%, RQ = 1). MMP-1 expression shows increased sensitivity to FTI/FPP combination than to FTI alone. KRAS and FNTA expression levels are minimally affected by FTI and FPP exposure. Statistical analysis (ANOVA two factor without replication) indicates that gene expression was stable with *P*-values for rows: $P = 0.2519$ and columns: $P = 0.0418$. (**B**) RT-qPCR analysis of MMP and TIMP gene expression changes of the 143B/T6-4, 5, 7 clones are shown with reference to the parental 143B cell line (where all target values are 100%). (**C**) MMP-1 expression levels were validated by Western blot. (**D**) Stable MMP-1 RNAi down-regulation affect on trans-membrane invasion was compared between the parental and T6-(4, 5, 7) clones.

Alexa-647-Phalloidin staining of the stress fibres. Depth-coding visualized the lamellipodia area as relatively smooth border regions in comparison to the rest of the cell body. The boundaries were then traced (G) and areas numbered and quantized with MetaMorph software. Quantization of lamellipodia surface areas and containing MMP-1 pixels (Fig. 3B) show that FPP increases both lamellipodia formation and MMP-1 localization (Fig. 3B, ~24% and ~19%, respectively). The surface area of lamellipodia changed with FTI-276, as did the MMP-1 localization within lamellipodia (Fig. 3B). Results of combined FPP/FTI exposure indicate that while lamellipodia formation was partially restored (87%), the lamellipodia MMP-1 localization was not under the investigated time period. It was observed that FTI-276 results in depletion of MMP-1 in the lamellipodia area by 60% when compared to untreated cells (Fig. 3B). FPP was not able to rescue the delivery of MMP-1 to the cell periphery. The histograms demonstrate significant differences between pharmacologic agents for lamellipodia formation and for MMP-1 content (ANOVA, $P < 0.0001$). This result is in agreement with observed changes in extracellular MMP-1 protein levels and invasive behaviour of the sarcoma cells.

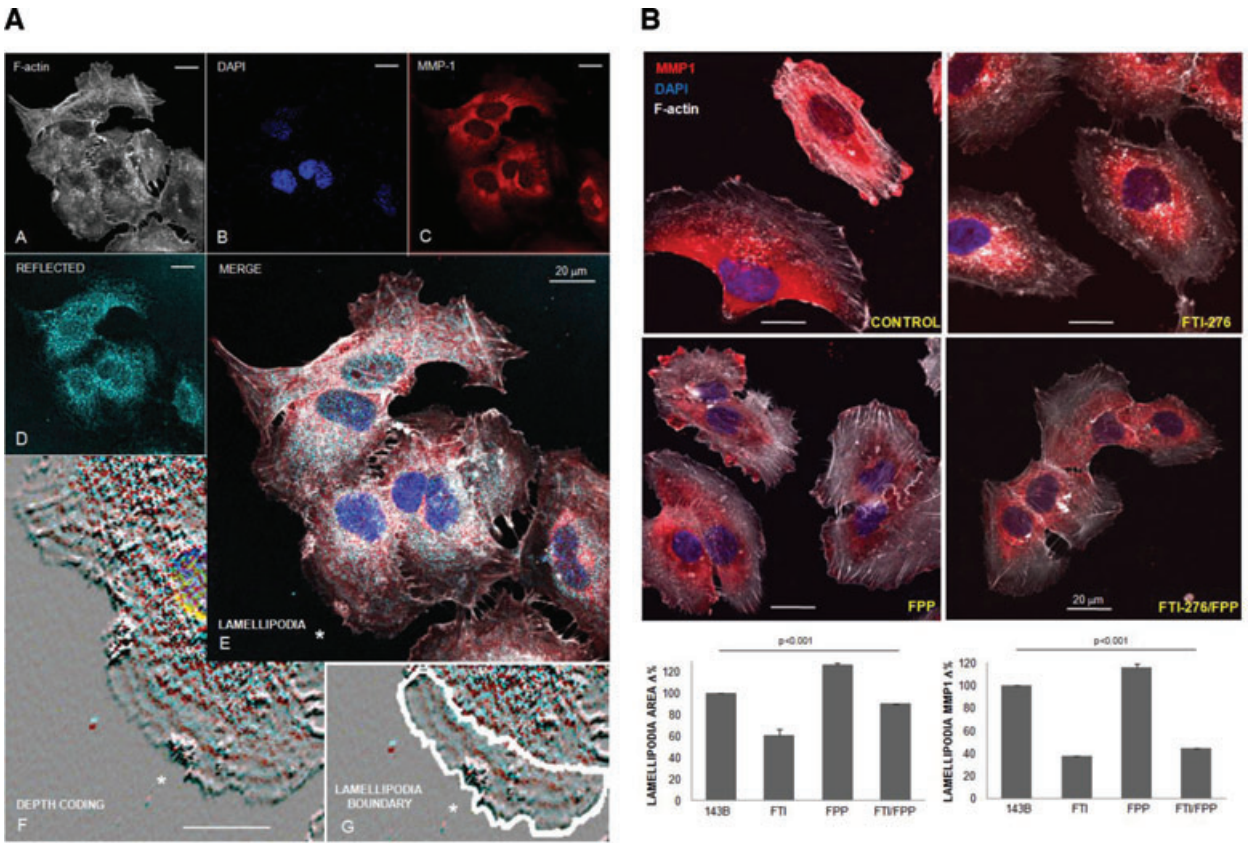

Fig. 3 Determination of MMP-1 lamellipodia localization. (**A**) Visual demonstration of objective invadopodia boundary determination through depth-coding. (**A**) Cellular architecture was outlined by Alexa-647-phalloidin staining (pseudo-coloured white) and aided by nuclear counterstaining with DAPI (B-blue). MMP-1 localization (C-red) and the reflected image (D-turquoise). The reflection image interference rings [E-Merge, labelled with asterisk (*)] delineate the stretched out regions of cellular bodies (lamellipodia) showing striped wave-like formations of protruding cellular frontlines. To demonstrate this phenomena more clearly, the interferential image was pseudo-coloured according to the height of cellular features (depth-coding, F). The boundaries of lamellipodia region circled (G-white). (**B**) MMP-1 delivery is FTI-276 sensitive. Fifteen to twenty randomly chosen fields of individual images (representing 60–90 individual cells) were captured of each condition with 63× oil immersion lens on the Zeiss LSM510 confocal microscope. Blue (DAPI, nucleus), red (MMP-1), pseudo-coloured white (F-actin) and reflected interference images (not shown) were collected. MetaMorph analysis was performed on the extracted red channels for total and partial surface areas and pixel counts to determine the podia formation activity and its partial MMP-1 representation as described. Each cell total surface area and MMP-1 content treated as fixed (100%). From this the lamellipodia formation and partial MMP-1 localization were determined as percentage of total values (surface area and red pixel counts). These percentage results presented as bar graph, where untreated cells provide the reference basis = 100% showing for drugs affecting lamellipodia surface area (bar graph on the left) and MMP-1 loading (bar graph on the right). Statistical analysis shows that the quantization of lamellipodia area and MMP-1 loading are different for and by the presented conditions with $P = 4.09E-73$ and $P = 5.60786E-30$ confidence levels, respectively.

Invadopodia MMP-1 activity levels are decreased by FTI

General paradigm is that MMP-1 secreted and deposited in the extracellular matrix as an inactive zymogen by various cell types where it is subsequently activated [47]. To investigate further if MMP-1 cellular production and localization can overlap with the underlying collagen matrix degradation beneath the cells, live cell fluorescent imaging in combination with DQ-collagen, MMP1-DsRed fusion protein expression and MMP-1 cleavage specific Fluorogenic Substrate-III (Fig. 4A and B; Refs. [48, 49]) were used in invadopodia assays.

Firstly, we confirmed that MMP1–DsRed fusion protein production and matrix degradation can be co-localized. DQ collagen (Fig. 4A, green, middle panel) shows matrix underlayment degradation (live cell images) which partially overlaps with MMP1–DsRed production and cellular localization (Fig. 4A, red, middle panel; three representative fields are shown). The data indicate that MMP1–DsRed expression (red) can be co-localized

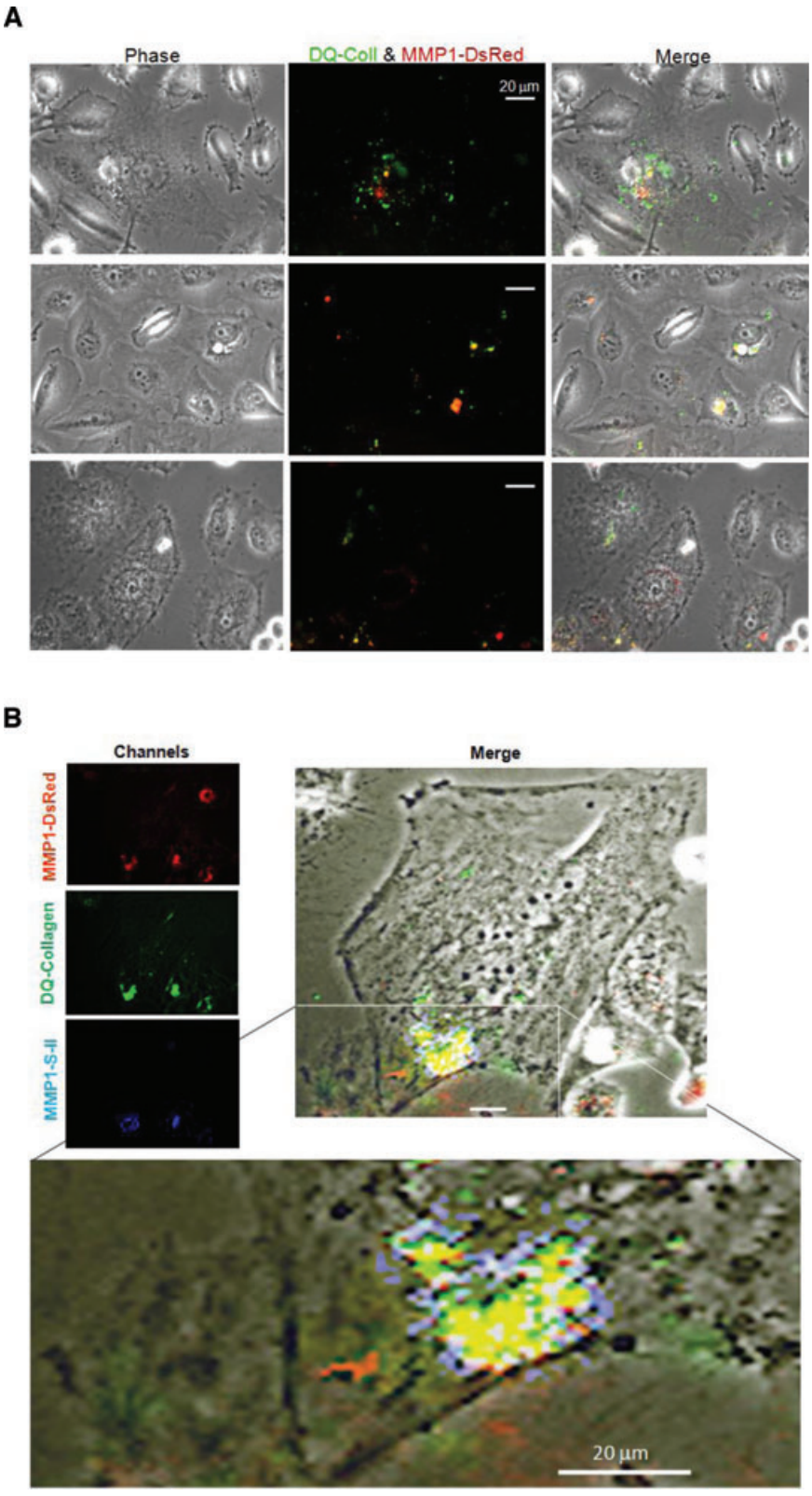

Fig. 4 MMP-1 directional trafficking into invadopodia regions. (**A**) 143B cells were seeded in 12-well plates at 3.0×10^4 concentrations. The live cell-related matrix degradation and MMP1-DsRed fusion construct production was imaged between 24 and 36 hrs from the DNA transfection. Except the DsRed fusion protein (constant fluorescence signal), the DQ-collagen becomes fluorescent upon enzymatic cleavage and degradation (three representative fields are shown, bar: 20 μm). (**B**) Images of MMP-1-DsRed transfected live cells. The data show that all fluorescent signal (green, red, blue,) demonstrate partial co-localization (inset), with white pixels where all three is simultaneously present (bars 20 μm).

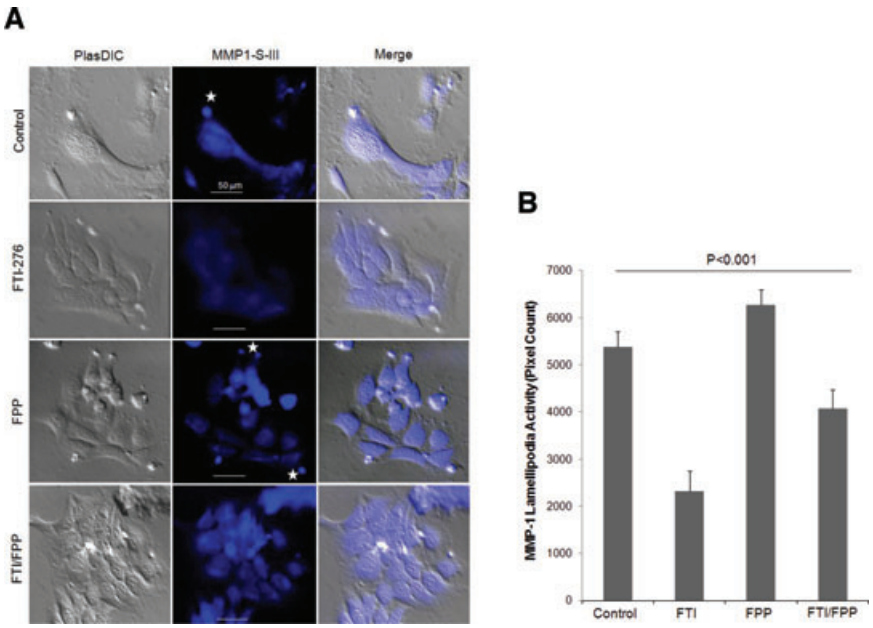

Fig. 5 MMP-1 activity is affected by farnesyl transferase inhibitor. (**A**) The lamellipodia regions were determined with polarized light and plastic optimized dichroic filter (PlasDIC). MMP-1 enzyme activity was detected by quenched Fluorogenic MMP1-Substrate-III (blue fluorescence indicates MMP-1 specific cleavage). The signals collected in the blue channel at ~λ = 460 nm, and up to 12 images of each condition (~25–30 cells). Five-pointed star labels MMP-1 activity localized to the podia regions of the cells. (**B**) Lamellipodia MMP-1 activities were quantized on 20 randomly selected cells in triplicate.

with degradation (green), creating yellow signals. Parallel, both can also observe in separate populations in Figure 4A (middle panel).

Secondly, because the DQ-collagen is not MMP-1 specific, we extended this result one step further. MMP-1 cleavage specific Fluorogenic Substrate-III was additively also incorporated into the underlying gel structures for live cell imaging. Result in Figure 4B shows that the expressed MMP1–DsRed fluorescent fusion construct (red) co-localized with the strong DQ-collagen degradation signal (green) in the invadopodia (yellow), which was incorporated also the MMP-1 cleavage specific Fluorogenic Substrate-III signal (blue, and white, where all three overlaps). Effect of pharmacologic inhibition of prenylation on MMP-1 activity (endogenously produced by the cells, no MMP-1 transfection) was examined and verified using only the MMP-1 cleavage specific Fluorogenic Substrate-III (Fig. 5; 49). Standardized gel thickness was established as described in the 'Materials and methods' section. As shown on the live cell images (Fig. 5A), lightly coloured regions in the untreated control (PlasDIC) correspond to strong MMP-1 enzymatic activity (blue in MMP1-S-III, indicated with white star). FTI-276 decreased overall MMP-1 activity and eliminated peripheral foci of degradation which is in agreement with the Western blotting results. Lamellipodia structures in the presence of FTI-276 are associated with less collagenase activity when compared to control or FPP treated cell population (MMP1-S-III, merged Fig. 5A). It should be noted that effective invasion depends on lamellipodia-localized MMP-1 enzymatic activity (Fig. 5B). Data of invadopodia quantization indicate a 57% activity down-regulation by FTI-276, which was partially restored by FPP with an increase to 75.8% all compared to untreated control podia region (pixel counts 100%).

Discussion

The current manuscript builds on the previous observations implicating the involvement of MMP-1 in sarcoma metastasis and the prenylation dependence of MMP-1 secretion [38,50–56]. The results demonstrate that MMP-1 delivery is prenylation dependent and this may affect cellular invasion. The advantages of performing this study in an established cell line instead of primary sarcoma cells are include but not limited to standardized and uniform gene expressional, invasive and podia formation responses, better support for MetaMorph analysis. The disadvantage, that established cell line responses seldom reflect the complexity of primary cell populations and could be biased through the immortalization process. There are two major limitations in this study. Firstly, the used prenylation inhibition is too broad to determine the detailed molecular mechanism of MMP-1 directional trafficking. Secondly, the 143B cells over expressing Ras, which in theory might affect the analysis. Because Ras and FNTA relative quantity did not fluctuate significantly (less than 20% difference; Fig. 2A) by treatments and we used the Ras only to prove that FTI-276 was working, we are confident that Ras expression did not introduce experimental bias.

In the absence of a more selective inhibitor of intracellular MMP-1 specific trafficking, prenylation inhibitors represent a convenient way to investigate the subcellular distribution and delivery of MMP-1 to the extracellular space [31]. Interestingly, FPP reversed some, but not all of the changes induced by FTI-276 and did not reverse the cytosolic accumulation of Ras. This is consistent with only a partial reversal of FNTA activity when examining

molecular, morphologic and functional parameters. The mechanism involving Ras inhibition may or may not be directly related to MMP-1 delivery. There are reports of Ras regulation of MMP-2 activation and MMP-9 expression which lend support to the linkage between proteases and protein delivery, suggesting an involvement of prenylation [57,58]. Ras-transformed cells are sensitive to FTI-276 as a pharmacologic agent [59,60]. The effect of FTI-276 on MMP-1 gene expression was down-regulated by approximately 30%, which was less than the effect on cellular localization and invasion. Others have also observed a similar effect in other MMP molecules and in MMP-1, which suggests that additional mechanism may be involved [38,61]. Stable RNAi down-regulation of MMP-1 caused ~50% decrease in migratory capacity validating its role in directional transmembrane migration (Fig. 2B–D). Importantly, the slight up-regulation of MMP-14 (as a result of clonal selection) did not modify MMP-1 knockdown affect on cellular invasion. The MMP-14 levels gradually decreased in the clones (T6-4 $>$ T6-5 $>$ T6-7) and this observation did not correlate with the invasiveness patterns (Fig. 2D).

An extra limitation of the study is that all determinations were made after overnight incubation while direct prenylation inhibition occurs over the course of minutes to hours. As such, the relationship between the time course of inhibition and effects on protein trafficking and invasiveness remain unclear. Previous studies examining the effects of FTI-276 on tumour growth utilized a slow release and a sustained concentration and then documented a 58% reduction in tumour volume over 18 weeks [62]. Abeles *et al*. measured secretion of MMP-1 from rheumatoid synovium over a 24-hr time period. Others have reported negative effects of prenylation inhibition at 4 hrs, and statistically significant effects at 24 hrs [63]. Thus, the inhibition kinetics of MMP-1 secretion by FTI-276 is broadly consistent with the known biological processes related to farnesylated proteins. The fact that farnesylation regulates MMP-1 secretion at least in part at the level of mRNA expression suggests multiple reasons why the effect of FTI-276 on MMP-1 secretion may be delayed.

To migrate through the collagen-based invasion assay, cells must transverse 8 μm pores and must degrade fibrillar collagen gel in the process (invadopodia related activity). This report indicates that at least part of the ability to traverse this barrier is MMP-1 dependent and prenylation sensitive. By inhibiting prenylation, MMP-1 subcellular localization was altered and subsequent collagenase activity and invasion were decreased. Each of these processes was at least in part reversed by the inclusion of FPP which is an FNTA substrate and served as a prenylation inhibitor agonist [61]. The data demonstrate that MMP-1 directional trafficking and its local activation contributed to the invasion process (Fig. 4). It should be noted that (a) not all cells expressed the MMP1–DsRed fusion protein signal (being transiently transformed by the construct); (b) there was more DQ collagen degradation signal than co-localized (could be due to endogenously produced MMP-1 activity or other collagenases); (c) there were also MMP1-DsRed signals that did not show local activation (no green DQ-collagen or blue MMP1-S-III substrate associated with it).

Conclusion

This paper suggests that MMP-1 directional delivery is an important part of cellular invasiveness and mediated at least in part by prenylation-dependent pathways. In this regard, directional trafficking is separated from the general secretion process. The data demonstrates that controlling local lamelli- and invadopodia delivery of MMP-1 through drugs and other complimentary approaches regulate invasive capacity. Our results illustrate that manipulating directional delivery and can be a beneficial alternative to general metalloproteinase blocking approaches either alone or in combination with other drug treatments.

Acknowledgements

We are indebted to Dr. George McNamara and Andras Donaszi-Ivanov at the University of Miami Bio-Imaging Core for their assistance with confocal microscopy and MetaMorph analysis. We thank Dr. Emily S. Clark for help with the invadopodia assays and David Chyatte, Sara Garamszegi for their contribution to the initial prenylation inhibition data. This project was supported by ACR 66105H to N.G., NIH CA-66088Y grant to S.P.S. and by the WCA-66461Y grant to N.G. and S.P.S. Other support was provided by the Sylvester Comprehensive Cancer Center and by the University of Miami, Miller School of Medicine.

Authors' contributions

N.G. designed the experiments, performed the microscopy data analysis, invadopodia assays, and the final draft of the manuscript. S.P.G. generated the stable MMP-1 RNAi clones, performed the invasion assays, RT-qPCR amplification, western blotting and related data analysis. S.P.S. oversaw the collection of data and wrote the first draft of the paper. All authors read and approved the final manuscript.

Conflict of interest

The authors have no financial disclosures regarding the performance of the work or the preparation of the current manuscript, and declare no competing and conflict of interests.

References

1. **Jiang X, Dutton CM, Qi WN, *et al.*** siRNA mediated inhibition of MMP-1 reduces invasive potential of a human chondrosarcoma cell line. *J Cell Physiol*. 2005; 202: 723–30.
2. **Pei D.** Matrix metalloproteinases target protease-activated receptors on the tumour cell surface. *Cancer Cell*. 2005; 7: 207–8.
3. **Polette M, Clavel C, Cockett M, *et al.*** Detection and localization of mRNAs encoding matrix metalloproteinases and their tissue inhibitor in human breast pathology. *Invasion Metast*. 1993; 13: 31–7.
4. **Pritchard SC, Nicolson MC, Lloret C, *et al.*** Expression of matrix metalloproteinases 1, 2, 9 and their tissue inhibitors in stage II non-small cell lung cancer: implications for MMP inhibition therapy. *Oncol Rep*. 2001; 8: 421–4.
5. **Vachani A, Nebozhyn M, Singhal S, *et al.*** A 10-gene classifier for distinguishing head and neck squamous cell carcinoma and lung squamous cell carcinoma. *Clin Cancer Res*. 2007; 13: 2905–15.
6. **Chen WT, Wang JY.** Specialized surface protrusions of invasive cells, invadopodia and lamellipodia, have differential MT1-MMP, MMP-2, and TIMP-2 localization. *Ann N Y Acad Sci*. 1999; 878: 361–71.
7. **Zaman MH, Matsudaira P, Lauffenburger DA.** Understanding effects of matrix protease and matrix organization on directional persistence and translational speed in three-dimensional cell migration. *Ann Biomed Eng*. 2007; 35: 91–100.
8. **Zaman MH, Trapani LM, Sieminski AL, *et al.*** Migration of tumour cells in 3D matrices is governed by matrix stiffness along with cell-matrix adhesion and proteolysis. [erratum appears in Proc Natl Acad Sci USA. 2006 Sep 12;103(37):13897]. *Proc Natl Acad Sci USA*. 2006; 103: 10889–94.
9. **Jiang X, Dutton CM, Qi W, *et al.*** Inhibition of MMP-1 expression by antisense RNA decreases invasiveness of human chondrosarcoma. *J Orthop Res*. 2003; 21: 1063–70.
10. **Yuan J, Dutton CM, Scully SP.** RNAi mediated MMP-1 silencing inhibits human chondrosarcoma invasion. *J Orthop Res*. 2005; 23: 1467–74.
11. **Coussens LM, Fingleton B, Matrisian LM.** Matrix metalloproteinase inhibitors and cancer: trials and tribulations. *Science*. 2002; 295: 2387–92.
12. **Overall CM, Lopez-Otin C.** Strategies for MMP inhibition in cancer: innovations for the post-trial era. *Nat Rev Cancer*. 2002; 2: 657–72.
13. **Vihinen P, Ala-aho R, Kahari VM.** Matrix metalloproteinases as therapeutic targets in cancer. *Curr Cancer Drug Targets*. 2005; 5: 203–20.
14. **Fisher JF, Mobashery S.** Recent advances in MMP inhibitor design. *Cancer Metast Rev*. 2006; 25: 115–36.
15. **Friedl P.** Dynamic imaging of cancer invasion and metastasis: principles and preclinical applications. *Clin Exp Metast*. 2009; 26: 269–71.
16. **Friedl P, Wolf K.** Proteolytic interstitial cell migration: a five-step process. *Cancer Metast Rev*. 2009; 28: 129–35.
17. **Friedl P, Wolf K.** Tumour-cell invasion and migration: diversity and escape mechanisms. *Nat Rev Cancer*. 2003; 3: 362–74.
18. **Wolf K, Friedl P.** Functional imaging of pericellular proteolysis in cancer cell invasion. *Biochimie*. 2005; 87: 315–20.
19. **Wolf K, Friedl P.** Mapping proteolytic cancer cell-extracellular matrix interfaces. *Clin Exp Metast*. 2009, 26: 289–98.
20. **Wolf K, Wu YI, Liu Y, *et al.*** Multi-step pericellular proteolysis controls the transition from individual to collective cancer cell invasion. *Nat Cell Biol*. 2007; 9: 893–904.
21. **Magee AI, Seabra MC.** Are prenyl groups on proteins sticky fingers or greasy handles? *Biochem J*. 2003; 376: e3–4.
22. **Bergo MO, Leung GK, Ambroziak P, *et al.*** Isoprenylcysteine carboxyl methyltransferase deficiency in mice. *J Biol Chem*. 2001; 276: 5841–5.
23. **Casey PJ, Seabra MC.** Protein prenyltransferases. *J Biol Chem*. 1996; 271: 5289–92.
24. **Seabra MC, Reiss Y, Casey PJ, *et al.*** Protein farnesyltransferase and geranylgeranyltransferase share a common alpha subunit. *Cell*. 1991; 65: 429–34.
25. **Mor A, Philips MR.** Compartmentalized Ras/MAPK signaling. *Annu Rev Immunol*. 2006; 24: 771–800.
26. **Caraglia M, Santini D, Marra M, *et al.*** Emerging anti-cancer molecular mechanisms of aminobisphosphonates. *Endocr Relat Cancer*. 2006; 13: 7–26.
27. **Konstantinopoulos PA, Karamouzis MV, Papavassiliou AG.** Post-translational modifications and regulation of the RAS superfamily of GTPases as anticancer targets. *Nat Rev Drug Discov*. 2007; 6: 541–55.
28. **Konstantinopoulos PA, Papavassiliou AG.** Multilevel modulation of the mevalonate and protein-prenylation circuitries as a novel strategy for anticancer therapy. *Trends Pharmacol Sci*. 2007; 28: 6–13.
29. **Yuasa T, Kimura S, Ashihara E, *et al.*** Zoledronic acid—a multiplicity of anti-cancer action. *Curr Med Chem*. 2007; 14: 2126–35.
30. **Bialek-Wyrzykowska U, Bauer BE, Wagner W, *et al.*** Low levels of Ypt protein prenylation cause vesicle polarization defects and thermosensitive growth that can be suppressed by genes involved in cell wall maintenance. *Mol Microbiol*. 2000; 35: 1295–311.
31. **Lantry LE, Zhang Z, Crist KA, *et al.*** Chemopreventive efficacy of promising farnesyltransferase inhibitors. *Exp Lung Res*. 2000; 26: 773–90.
32. **Hassan M, Feyen O, Grinstein E.** Fas-induced apoptosis of renal cell carcinoma is mediated by apoptosis signal-regulating kinase 1 *via* mitochondrial damage-dependent caspase-8 activation. *Cell Oncol*. 2009; 31: 437–56.
33. **Clark MK, Scott SA, Wojtkowiak J, *et al.*** Synthesis, biochemical, and cellular evaluation of farnesyl monophosphate prodrugs as farnesyltransferase inhibitors. *J Med Chem*. 2007; 50: 3274–82.
34. **Jabbour E, Kantarjian H, Cortes J.** Clinical activity of farnesyl transferase inhibitors in hematologic malignancies: possible mechanisms of action. *Leuk Lymphoma*. 2004; 45: 2187–95.
35. **Sebti SM, Hamilton AD.** Anticancer activity of farnesyltransferase and geranylgeranyltransferase I inhibitors: prospects for drug development. *Expert Opin Investig Drugs*. 1997; 6: 1711–4.
36. **Sousa SF, Fernandes PA, Ramos MJ.** Farnesyltransferase inhibitors: a detailed chemical view on an elusive biological problem. *Curr Med Chem*. 2008; 15: 1478–92.
37. **Winter-Vann AM, Casey PJ.** Post-prenylation-processing enzymes as new targets in oncogenesis. *Nat Rev Cancer*. 2005; 5: 405–12.
38. **Abeles AM, Marjanovic N, Park J, *et al.*** Protein isoprenylation regulates secretion of matrix metalloproteinase 1 from rheumatoid synovial fibroblasts: effects of statins and farnesyl and geranylgeranyl

transferase inhibitors. [erratum appears in Arthritis Rheum. 2007 Oct;56(10):3510 Note: Al-Mussawir, Hayfez [corrected to Al-Mussawir, Hayf E]]. *Arthritis Rheumat*. 2007; 56: 2840–53.

39. **Cole SL, Grudzien A, Manhart IO, *et al.*** Statins cause intracellular accumulation of amyloid precursor protein, beta-secretase-cleaved fragments, and amyloid beta-peptide *via* an isoprenoid-dependent mechanism. *J Biol Chem*. 2005; 280: 18755–70.
40. **Michaelson D, Ahearn I, Bergo M, *et al.*** Membrane trafficking of heterotrimeric G proteins *via* the endoplasmic reticulum and Golgi. *Mol Biol Cell*. 2002; 13: 3294–302.
41. **Modiano N, Lu YE, Cresswell P.** Golgi targeting of human guanylate-binding protein-1 requires nucleotide binding, isoprenylation, and an IFN-gamma-inducible cofactor. *Proc Natl Acad Sci USA*. 2005; 102: 8680–5.
42. **Stickney JT, Booden MA, Buss JE.** Targeting proteins to membranes, using signal sequences for lipid modifications. *Methods Enzymol*. 2001; 332: 64–77.
43. **Alexander NR, Branch KM, Parekh A, *et al.*** Extracellular matrix rigidity promotes invadopodia activity. *Curr Biol*. 2008; 18: 1295–9.
44. **Clark ES, Weaver AM.** A new role for contacting in invadopodia: regulation of protease secretion. *Eur J Cell Biol*. 2008; 87: 581–90.
45. **Clark ES, Whigham AS, Yarbrough WG, *et al.*** Cortactin is an essential regulator of matrix metalloproteinase secretion and extracellular matrix degradation in invadopodia. *Cancer Res*. 2007; 67: 4227–35.
46. **Guida WC, Hamilton AD, Crotty JW, *et al.*** Protein farnesyltransferase: flexible docking studies on inhibitors using computational modeling. *J Comp-Aided Molec Design*. 2005; 19: 871–85.
47. **Seiki M.** Membrane-type 1 matrix metalloproteinase: a key enzyme for tumour invasion. *Cancer Lett*. 2003; 194: 1–11.
48. **Yan SJ, Blomme EA.** *In situ* zymography: a molecular pathology technique to l ocalize endogenous protease activity in tissue sections. *Vet Pathol*. 2003; 40: 227–36.
49. **McGeehan GM, Bickett DM, Green M, *et al.*** Characterization of the peptide substrate specificities of interstitial collagenase and 92-kDa gelatinase. Implications for substrate optimization. *J Biol Chem*. 1994; 269: 32814–20.
50. **Yuan J, Dutton CM, Scully SP.** RNAi mediated MMP-1 silencing inhibits human chondrosarcoma invasion. *J Orthop Res*. 2005; 23: 1467–74.
51. **Jiang X, Dutton CM, Qi WN, *et al.*** siRNA mediated inhibition of MMP-1 reduces invasive potential of a human chondrosarcoma cell line. *J Cell Physiol*. 2005; 202: 723–30.
52. **Fong YC, Dutton CM, Cha SS, *et al.*** Absence of a correlation between the presence of a single nucleotide polymorphism in the matrix metalloproteinase 1 promoter and outcome in patients of chondrosarcoma. *Clin Cancer Res*. 2004; 10: 7329–34.
53. **Jiang X, Dutton CM, Qi W, *et al.*** Inhibition of MMP-1 expression by antisense RNA decreases invasiveness of human chondrosarcoma. *J Orthop Res*. 2003; 21: 1063–70.
54. **Scully SP, Berend KR, Toth A, *et al.*** Marshall Urist Award. Interstitial collagenase gene expression correlates with *in vitro* invasion in human chondrosarcoma. *Clin Orthop Relat Res*. 2000: 291–303.
55. **Scully SP, Berend KR, Qi WN, *et al.*** Collagenase specificity in chondrosarcoma metastasis. *Braz J Med Biol Res*. 1999; 32: 885–9.
56. **Berend KR, Toth AP, Harrelson JM, *et al.*** Association between ratio of matrix metalloproteinase-1 to tissue inhibitor of metalloproteinase-1 and local recurrence, metastasis, and survival in human chondrosarcoma. *J Bone Joint Surg Am*. 1998; 80: 11–7.
57. **Kim IY, Jeong SJ, Kim ES, *et al.*** Type I collagen-induced pro-MMP-2 activation is differentially regulated by H-Ras and N-Ras in human breast epithelial cells. *J Biochem Mol Biol*. 2007; 40: 825–31.
58. **Lee KW, Kim MS, Kang NJ, *et al.*** H-Ras selectively up-regulates MMP-9 and COX-2 through activation of ERK1/2 and NF-kappaB: an implication for invasive phenotype in rat liver epithelial cells. *Int J Cancer*. 2006; 119: 1767–75.
59. **Sun J, Qian Y, Hamilton AD, *et al.*** Ras CAAX peptidomimetic FTI 276 selectively blocks tumour growth in nude mice of a human lung carcinoma with K-Ras mutation and p53 deletion. *Cancer Res*. 1995; 55: 4243–7.
60. **Lerner EC, Qian Y, Blaskovich MA, *et al.*** Ras CAAX peptidomimetic FTI-277 selectively blocks oncogenic Ras signaling by inducing cytoplasmic accumulation of inactive Ras-Raf complexes. *J Biol Chem*. 1995; 270: 26802–6.
61. **Kang S, Kim ES, Moon A.** Simvastatin and lovastatin inhibit breast cell invasion induced by H-Ras. *Oncol Rep*. 2009; 21: 1317–22.
62. **Lantry LE, Zhang Z, Yao R, *et al.*** Effect of farnesyltransferase inhibitor FTI-276 on established lung adenomas from A/J mice induced by 4-(methylnitrosamino)-1-(3-pyridyl)-1-butanone. *Carcinogenesis*. 2000; 21: 113–6.
63. **Reuter CW, Morgan MA, Bergmann L.** Targeting the Ras signaling pathway: a rational, mechanism-based treatment for hematologic malignancies? *Blood*. 2000; 96: 1655–69.